Electronic Supplementary Material (ESI) for New Journal of Chemistry.

Fabricating 3D Ultra-thin N-doped Porous Graphene-like Catalysts Based on Polymerized Amino Acid Metal Chelates as Efficient Oxygen Electrocatalyst for Zn–air Batteries

Yunxiao Zhang[1,a,b], Wenhua Xiao[1,a], Yuan Yin[a], De Zheng Peng[a], Hongqiang Wang[b], Minjie Zhou[a], Zhaohui Hou[a], Yu Liu[a*], Binhong He[a*]

[a]*Key Laboratory of Hunan Province for Advanced Carbon–based Functional Materials, School of Chemistry and Chemical Engineering, Hunan Institute of Science and Technology, Yueyang 414006, Hunan, China*

[b]*Guangxi Key Laboratory of Low Carbon Energy Material, Guangxi Normal University, Guilin 541004, China*

[*]**Corresponding authors.**

Email addresses: hiliu2000@126.com (Y. Liu), 11990398@hnist.edu.cn (B. He)

[1] These authors contributed equally to this work.

Table of Contents

commercialized Pt/C electrodes at 0.72V in O_2 saturated 0.1 M KOH electrolyte before and after adding 3 M methanol.

Table S1 The XPS result of NPCs.

Table S2 The N 1s spectra fitting results of NPCs.

Table S3 The specific BET result of NPCs.

Table S4 Comparison of the ORR performance in 0.1M KOH solution between this work and some other works reported previously.

1.1 Materials characterization

Scanning electron microscope (SEM) was conducted with a field emission scanning electron microanalyzer (Hitachi S-4800, Japan). Transmission electron microscope (TEM) images were collected on a JEM-2100F with an EDX analytical system. Fourier transform infrared spectroscopy (FTIR) analysis was carried out on a Fourier transform infrared spectrometer (FTIR-5300). X-ray diffraction (XRD) patterns were recorded on a Philips PC-APD diffractometer operating at 40 kV and 60 mA using Cu Kα radiation (λ = 1.5418 Å). Raman spectroscopy was performed on a Labram-010 spectrometer ranging from 500 to 2000 cm^{-1}. Electrical conductivity was measured on a SZT-2 four-probe conductivity meter. X-ray photoelectron spectroscopy (XPS) analysis was carried out on an ESCALAB 250 spectrometer using a Mg Kα X-ray source.

1.2 Electrochemical measurements

1.2.1 ORR performance

4 mg of the NPCs or Pt/C catalyst (De Nora Elettrodi Co. Ltd., 20 *wt*.% Pt on

carbon black) was dispersed into the mixture of 980 μL of ethanol and 20 μL of 5 *wt.*% Nafion solution, and then ultrasonicated for 20 min to form homogeneous catalyst inks. Next, 20 μL of the catalyst ink was carefully dropped onto the polished glassy carbon rotating disk electrode. The electrochemical performance was tested in a typical three-electrode cell on the CHI 760E electrochemical workstation equipped with rotating disk electrode (RDE, Φ = 5 mm). The geometrical surface area of the disc electrode is 0.196 cm^2 and the catalyst loading is 0.4 mg cm^{-2}. A platinum foil and an Ag/AgCl electrode filled with saturated KCl aqueous solution were utilized as the counter and reference electrodes, respectively. The ORR activity was detected in O_2-saturated 0.1 M KOH solution by using a rotating disk electrode (Pine Instrument, MSR analytical rotator). The ORR kinetic parameters were analyzed by the following KoutechyLevich (K-L) equation:

$$\frac{1}{J}=\frac{1}{0.62nFC_0D_0^{2/3}\nu^{-1/6}\omega^{1/2}}+\frac{1}{J_k}$$

Where J is the tested current density, J_K means kinetic current density. n represents the electron transfer number, F refers to Faraday constant (96485 C mol^{-1}), C_0 is oxygen bulk concentration (1.2×10^{-3} M in 0.1 M KOH), D_0 is the oxygen diffusion coefficient (1.9×10^{-5} cm^2 s^{-1} in 0.1 M KOH), ν is electrolyte kinetic viscosity (0.01 cm^2 s^{-1}) and ω is disk angular velocity.

In basic electrolyte (0.1 M KOH), all potentials can be converted to reversible hydrogen electrode (RHE) by the following equation: $E_{RHE}=E_{Ag/AgCl}$ + 0.97 V. Cyclic voltammetry (CV) curve was tested in N_2 or O_2 saturated electrolyte within a voltage range from -0.2 to 1.2 V (*vs*. RHE) at a scan rate of 50 mV s^{-1}. Linear sweep

voltammetry (LSV) curve was measured at a scan rate of 10 mV s^{-1} at various rotation speeds from 400 to 1600 rpm within identical voltage range. The onset potential is determined by making a tangent line to the horizontal line and a tangent line to the descending slope, intersecting at a point at which the corresponding potential is the onset potential.

1.2.2 Zn-air batteries performance

Liquid Zn–air battery (ZAB) tests were conducted in home–made electrochemical cells. The air cathode consists of a hydrophobic carbon paper (3 cm×3 cm) with a gas diffusion layer on the air-facing side and a catalyst layer on the water-facing side. The loading amount for NPC–1050 or Pt/C catalyst (20 *wt*.% Pt on carbon black) is 0.9 mg cm^{-2} onto carbon paper warping the current collector (copper-foam). A polished Zn plate (3 cm×8 cm) as the anode. The electrolyte used for ZAB is 6 M KOH containing 0.2 M $Zn(Ac)_2$. ZAB were performed with homemade zinc-air battery using CHI 760E electrochemical workstation and LAND.

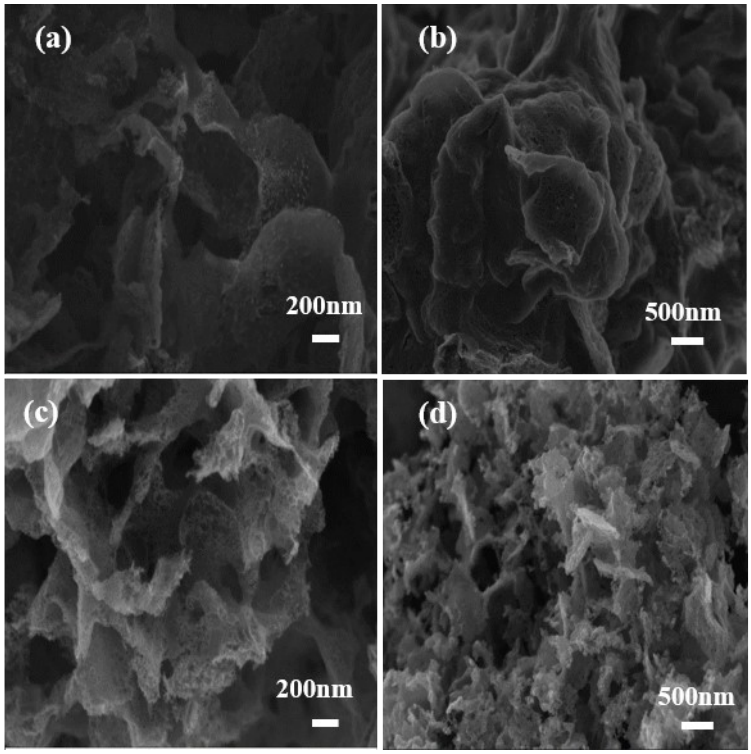

Figure S1 SEM images of (a,b) NPC–950 and (c,d) NPC–1150.

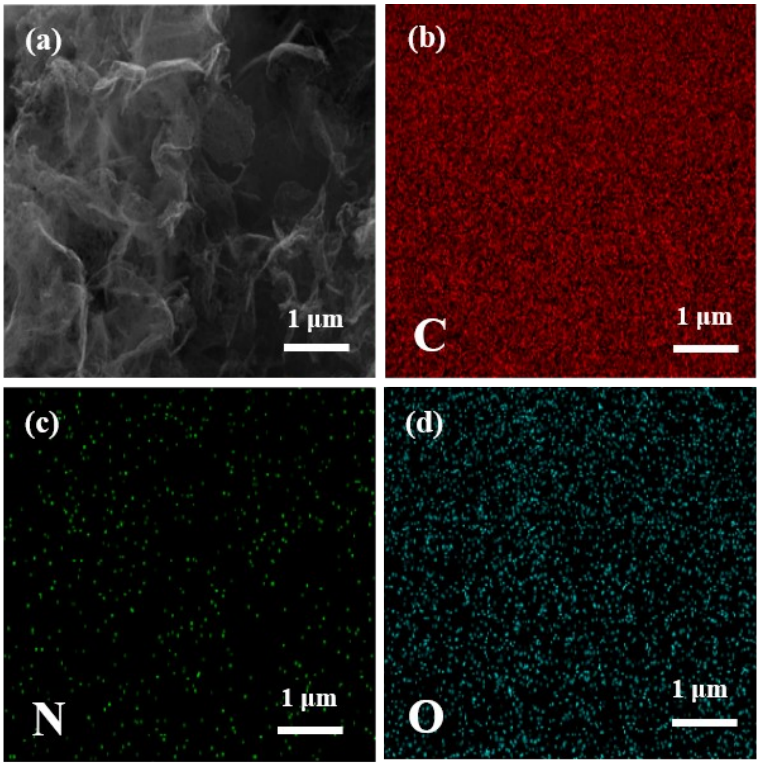

Figure S2 SEM image of (a)NPC–1050 and the corresponding elemental mapping images of (b) carbon, (c) nitrogen and (d) oxygen.

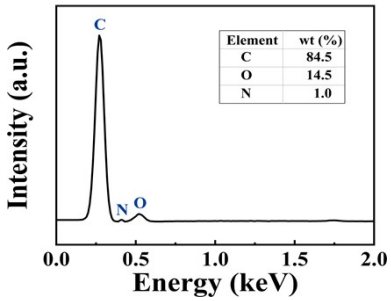

Figure S3 The EDS spectra of NPC–1050 catalyst.

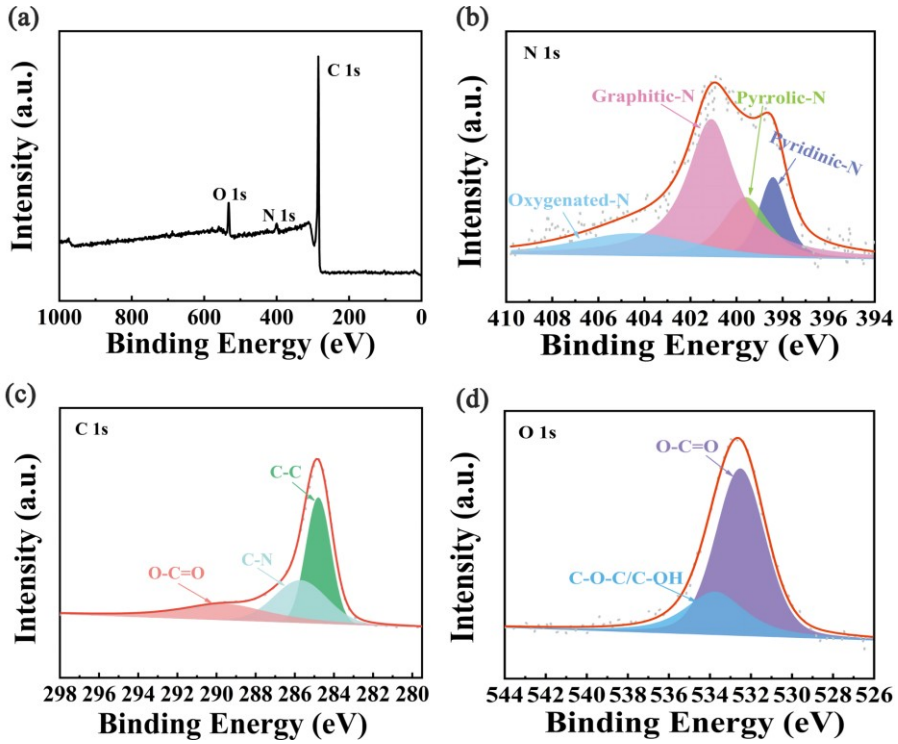

Figure S4 (a) XPS full scan, (b) N 1s XPS spectrum, (c) C 1s XPS spectrum and (d) O 1s XPS spectrum of NPC–950.

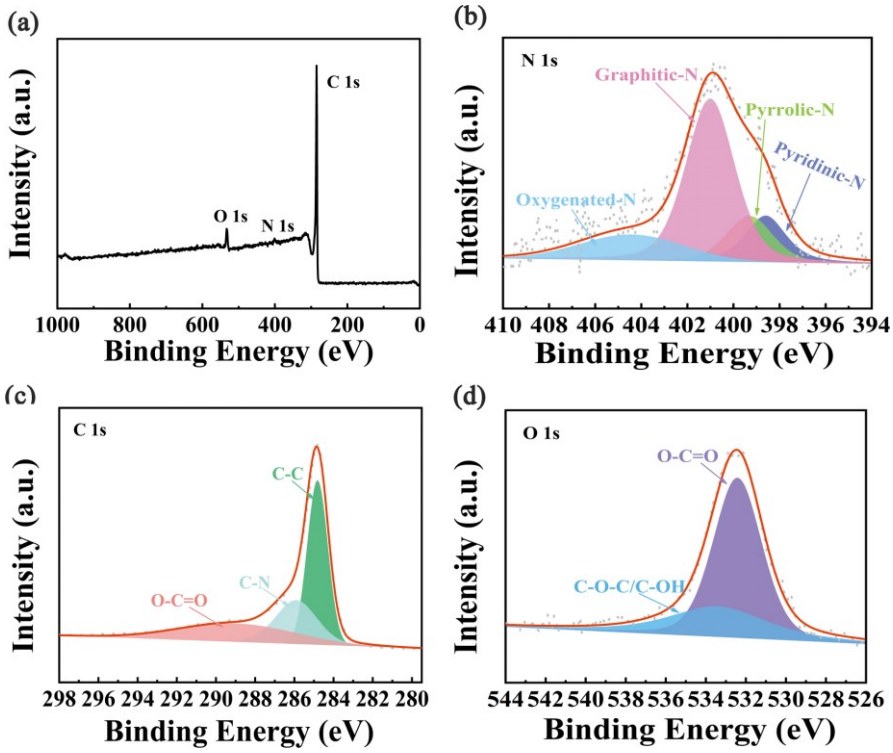

Figure S5 (a) XPS full scan, (b) N 1s XPS spectrum, (c) C 1s XPS spectrum and (d) O 1s XPS spectrum of NPC–1150.

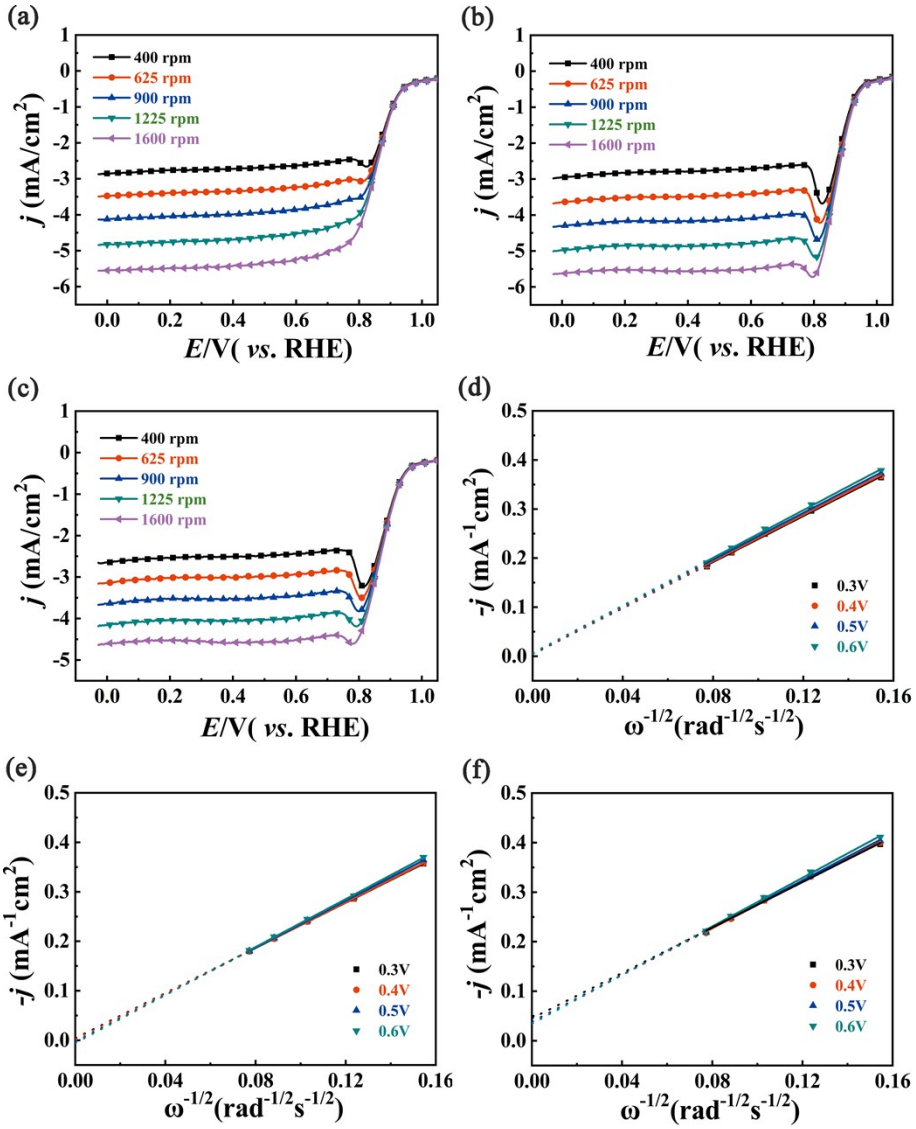

Figure S6 LSV curves at different rotating speeds for (a) NPC–950, (b) NPC–1050, (c) NPC–1150 in O_2-saturated 0.1 M KOH electrolyte (scan rate: 10 mV s^{-1}). K-L plots at various potential for (d) NPC–950, (e) NPC–1050, (f) NPC–1150, in O_2-saturated 0.1 M KOH electrolyte.

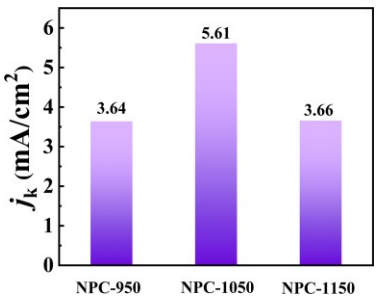

Figure S7 J_k at 0.85 V of NPCs at different pyrolysis temperatures.

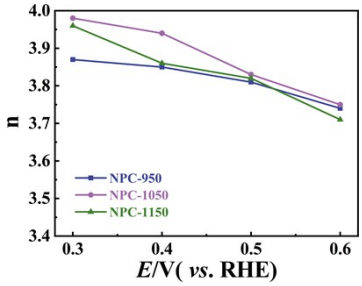

Figure S8 The number of transferred electrons of NPCs.

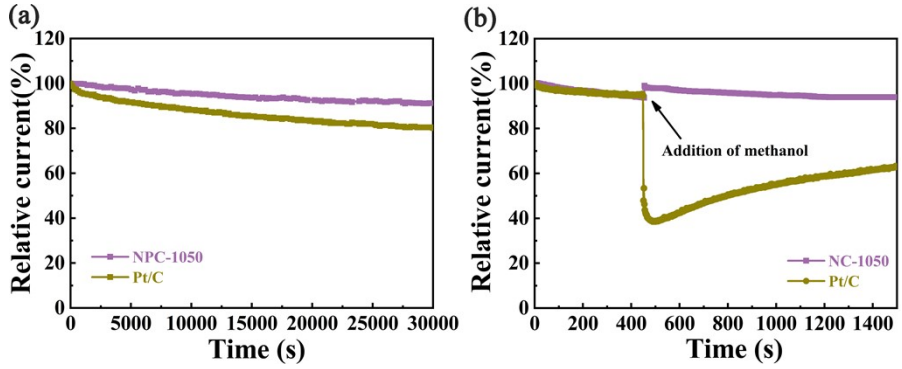

Figure S9 (a) The relative current density vs. time plot on NPC–1050 and commercialized Pt/C electrodes at 0.72 V for 30000 s in O_2 saturated 0.1 M KOH electrolyte. (b) The relative current density vs. time plots on NPC–1050 and commercialized Pt/C electrodes at 0.72V in O_2 saturated 0.1 M KOH electrolyte before and after adding 3 M methanol.

Table S1. The XPS result of NPCs.

Samples	C (*at. %*)	N (*at. %*)	O (*at. %*)
NPC–950	88.89	3.84	7.27
NPC–1050	92.62	2.63	4.74
NPC–1150	93.07	2.24	4.68

Table S2. The N 1s spectra fitting results of NPCs.

Samples	Pyridinic–N (%)	Pyrrolic–N (%)	Graphitic–N (%)	Oxygenated–N (%)
NPC–950	14.23	17.26	51.34	17.17
NPC–1050	17.13	15.46	53.24	14.16
NPC–1150	14.72	14.65	54.52	16.11

Table S3. The specific BET result of NPCs samples.

Samples	Specific Surface Area (m^2g^{-1})	Pore Volume (cm^3g^{-1})	Pore Size (nm)
NPC–950	1321.75	1.79	7.01
NPC–1050	1501.00	1.62	5.87
NPC–1150	1334.35	1.80	7.81

Table S4. Comparison of the ORR performance in 0.1M KOH solution between this work and some other works reported previously.

Samples	E_{onset} (V vs. RHE)	$E_{1/2}$ (V *vs*. *RHE*)	J_L (mA cm^{-2})	Transfer number (n)	loading mass (mg cm^{-2})	References
NPC–1050	**0.970**	**0.878**	**5.64**	**3.88**	**0.40**	**This work**
CMP–NP–900	0.930	0.857	-	3.96	0.31	**S1**
JCNT–0.5	0.97	0.88	5.85	4.0	0.4	**S2**
PANRGO–700	-	0.864	-	3.96	0.20	**S3**
NCF	1.0	0.85	5.9	3.85	0.20	**S4**
NPC–1000	0.90	0.82	-	3.70	0.43	**S5**
N–CNSP	0.96	0.85	6.1	4.00	0.51	**S6**
NCD 1000	0.96	0.86	5.74	3.8	0.25	**S7**
CF	1.02	0.87	~4	3.4~3.8	0.25	**S8**
HNCSs	0.92	0.82	5.34	3.86	0.20	**S9**

References

[S1] H. Sun, P. Zhou, X. Ye, J. Wang, Z. Tian, Z. Zhu, C. Ma, W. Liang, A. Li, Nitrogen-doping hollow carbon nanospheres derived from conjugated microporous polymers toward oxygen reduction reaction, J Colloid Interface Sci 617 (2022) 11-19.

[S2] C. Jin, H. Deng, J. Zhang, Y. Hao, J. Liu, Jagged carbon nanotubes from polyaniline: Strain-driven high-performance for Zn-air battery, Chemical Engineering Journal 434 (2022).

[S3] H. Begum, M.S. Ahmed, S. Jung, Template-free synthesis of polyacrylonitrile-derived porous carbon nanoballs on graphene for efficient oxygen reduction in zinc–air batteries, Journal of Materials Chemistry A 9(15) (2021) 9644-9654.

[S4] L. Zhang, T. Gu, K. Lu, L. Zhou, D.S. Li, R. Wang, Engineering Synergistic Edge-N Dipole in Metal-Free Carbon Nanoflakes toward Intensified Oxygen Reduction Electrocatalysis, AFM 31(42) (2021).

[S5] B. Guo, R. Ma, Z. Li, S. Guo, J. Luo, M. Yang, Q. Liu, T. Thomas, J. Wang, Hierarchical N-doped porous carbons for Zn–Air batteries and supercapacitors, Nano-micro letters 12(1) (2020) 1-13.

[S6] L. Zong, W. Wu, S. Liu, H. Yin, Y. Chen, C. Liu, K. Fan, X. Zhao, X. Chen, F. Wang, Y. Yang, L. Wang, S. Feng, Metal-free, active nitrogen-enriched, efficient bifunctional oxygen electrocatalyst for

ultrastable zinc-air batteries, Energy Storage Materials 27 (2020) 514-521.
[S7] Q. Lai, J. Zheng, Z. Tang, D. Bi, J. Zhao, Y. Liang, Optimal Configuration of N-Doped Carbon Defects in 2D Turbostratic Carbon Nanomesh for Advanced Oxygen Reduction Electrocatalysis, Angew Chem Int Ed Engl 59(29) (2020) 11999-12006.
[S8] J. Gao, Y. Wang, H. Wu, X. Liu, L. Wang, Q. Yu, A. Li, H. Wang, C. Song, Z. Gao, M. Peng, M. Zhang, N. Ma, J. Wang, W. Zhou, G. Wang, Z. Yin, D. Ma, Construction of a sp(3) /sp(2) Carbon Interface in 3D N-Doped Nanocarbons for the Oxygen Reduction Reaction, Angew Chem Int Ed Engl 58(42) (2019) 15089-15097.
[S9] L. Chai, L. Zhang, X. Wang, L. Xu, C. Han, T.-T. Li, Y. Hu, J. Qian, S. Huang, Bottom-up synthesis of MOF-derived hollow N-doped carbon materials for enhanced ORR performance, Carbon 146 (2019) 248-256.